Electronic Supplementary Material (ESI) for Physical Chemistry Chemical Physics

Electronic Supporting Information

for

Nonadiabatic Decay Dynamics of 9*H*-Guanine in Aqueous Solution

Berit Heggen,[a] Zhenggang Lan,[b] and Walter Thiel[a]

[a] Max-Planck-Institut für Kohlenforschung, Kaiser-Wilhelm-Platz 1, 45470 Mülheim an der Ruhr, Germany, E-mail: thiel@mpg-muelheim.mpg.de

[b] Qingdao Institute of Bioenergy and Bioprocess Technology, Chinese Academy of Science, Qingdao, 226101, P. R. China, E-mail: lanzg@qibebt.ac.cn

1 Absorption spectrum

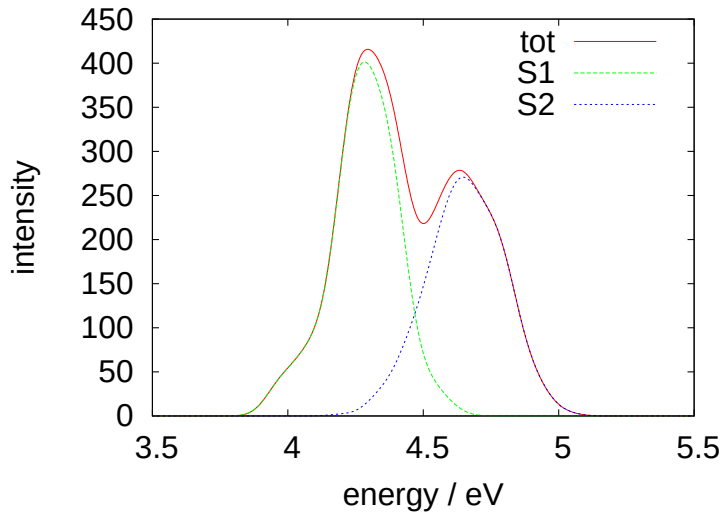

Figure 1: Calculated absorption spectrum of 9*H*-guanine in aqueous solution. Color code: red, full absorption spectrum; green, contribution from excitation to S_1; blue, contribution from excitation to S_2.

2 Energies for 9*H*-guanine in vacuo

Table 1: State energies (eV) at the indicated gas-phase minima relative to the ground-state minimum

	Geom	S_0	S_1	S_2	S_3
Gas	$(S_0)_{min}$	0.00	4.26	4.99	5.33
Phase	$(S_{1\alpha})_{min}$	3.15	3.19	-	-
	$(S_{1\beta})_{min}$	1.83	3.37	5.52	5.59
	CI_α	3.52	3.52	6.10	6.52
	CI_β	3.16	3.16	5.63	6.05
	CI_γ	3.20	3.20	5.90	6.13

3 Comparison of gas phase geometries

In this section we compare optimized gas phase geometries of groundstate and excited-state minima as well as conical intersections of 9*H*-guanine, obtained by Lan *et. al.* using OM2/MRCI (Reference 31) and by Barbatti *et. al.* using the *ab initio* MRCIS method (Reference 32). We present selected bond lengths, bond angles, and dihedral angles (Table 2) as well as Cremer-Pople parameters for the distortion of the six-membered ring (Table 3). In addition, we show overlays of the OM2/MRCI and *ab initio* MRCIS structures (Figure 2).

We now comment on similarities and differences between the OM2/MRCI and MRCIS geometries. It is obvious from Figure 2 that the structures of the five-membered rings generally match very well. The ground-state structures $\mathbf{(S_0)}_{min}$ resemble each other closely, except for a slight pyramidalization of the amino group (MRCIS) that is not observed at the semiempirical level (OM2/MRCI). In all other structures, there are more or less pronounced out-of-plane distortions in the six-membered ring which may occur in upward or downward direction (leading to pairs of enantiomers that differ in the sign of out-of-plane dihedral angles). Table 2 contains the raw dihedral angles as obtained from the OM2/MRCI and MRCIS geometry optimizations (which may correspond to different enantiomers). When generating the overlays shown in Figure 2, care was taken to superimpose the same enantiomers with analogous dihedral angles; this was ensured in practice by inverting, if necessary, the sign of all *z*-coordinates in the OM2/MRCI geometries.

In the case of the excited-state minimum $\mathbf{(S_{1,\alpha})}_{min}$, the overall shape of both structures is rather similar (Figure 2b), but the bond lengths vary more strongly for MRCIS, with the C5-C6 bond elongated and the C6-O6 bond shortened by 0.1 Å relative to OM2/MRCI (Table 2). The two $\mathbf{(S_{1,\beta})}_{min}$ ring structures are rather similar, with relatively minor deviations in key parameters (Table 2); however, the amino substituent shows a considerably stronger out-of-plane displacement for MRCIS, accompanied by a boat-like distortion of the six-membered ring (Figure 2c).

Table 2: Selected bond lengths (Å), bond angles, and dihedral angles (degree) in the optimized gas-phase structures of the following 9*H*-guanine species: $(S_0)_{min}$, $(S_1)_{min}$, $CI_{01,\alpha}$, $CI_{01,\beta}$, and $CI_{01,\gamma}$. OM2/MRCI and MRCIS results from References 31 and 32, respectively.

	$(S_0)_{min}$		$(S_{1,\alpha})_{min}$		$(S_{1,\beta})_{min}$		$CI_{01,\alpha}$		$CI_{01,\beta}$		$CI_{01,\gamma}$	
	OM2	MRCIS	OM2	MRCIS	OM2	MRCIS	OM2	MRCIS	OM2	MRCIS	OM2	MRCIS
bonds /Å												
N1-C6	1.43	1.41	1.47	1.43	1.41	1.42	1.47	1.39	1.49	1.44	1.64	2.07
C4-C5	1.43	1.39	1.49	1.37	1.51	1.45	1.58	1.46	1.51	1.42	1.51	1.39
C5-C6	1.45	1.43	1.56	1.43	1.46	1.44	1.47	1.47	1.46	1.45	1.56	1.52
C6-O6	1.24	1.22	1.26	1.36	1.24	1.22	1.26	1.20	1.22	1.21	1.23	1.20
angles /°												
C2-N3-C4	113	113	113	113	110	102	112	99	109	105	114	115
C4-C5-C6	118	119	115	118	117	119	114	119	115	120	104	122
C5-C6-O6	131	131	107	123	127	127	133	126	117	127	119	116
C5-C6-N1	112	110	108	112	114	111	109	109	111	112	103	90
dihedrals /°												
C2-N3-C4-C5	0	-2	-27	-2	11	-18	-15	18	-28	27	29	-14
C4-C5-C6-O6	-180	179	-151	-148	165	-170	-151	154	173	177	61	-87
N3-C4-C5-N7	180	-179	-169	-178	176	-177	-169	-179	-149	171	176	-179
N2-C2-N1-C6	-180	178	166	170	-177	143	177	-144	97	-80	138	-131

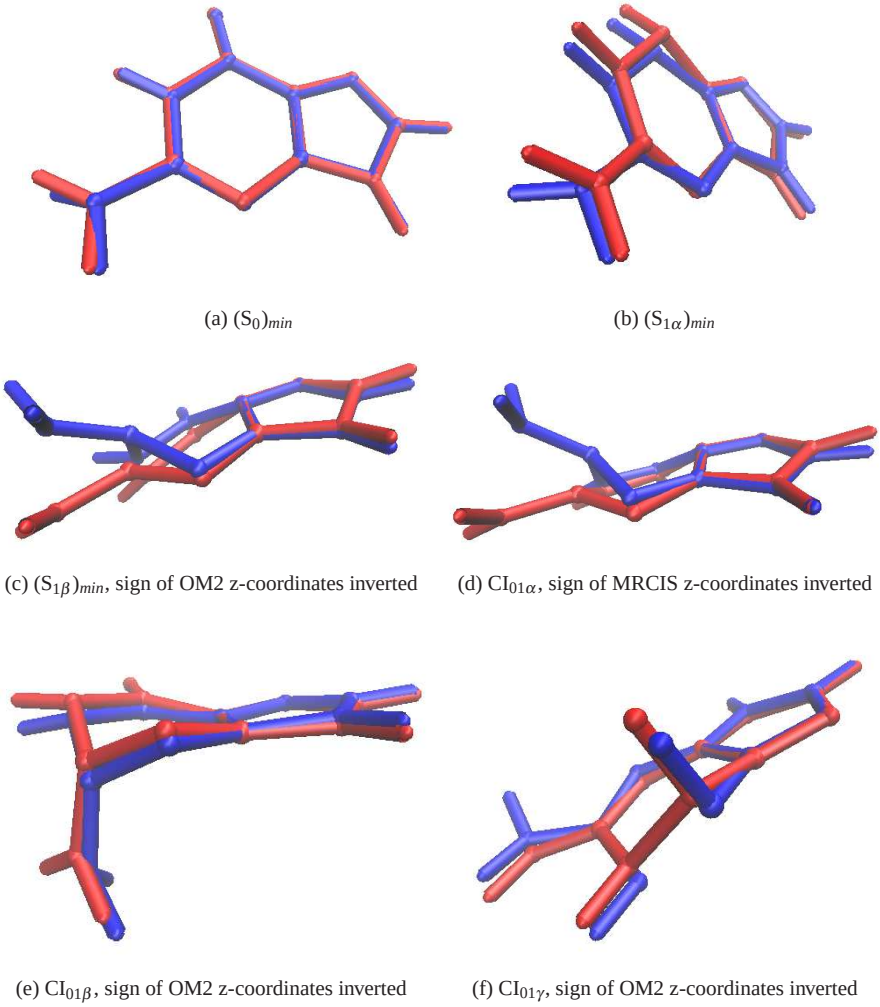

(a) $(S_0)_{min}$ (b) $(S_{1\alpha})_{min}$

(c) $(S_{1\beta})_{min}$, sign of OM2 z-coordinates inverted (d) $CI_{01\alpha}$, sign of MRCIS z-coordinates inverted

(e) $CI_{01\beta}$, sign of OM2 z-coordinates inverted (f) $CI_{01\gamma}$, sign of OM2 z-coordinates inverted

Figure 2: Overlay of optimized gas phase geometries from OM2/MRCI (red) and *ab initio* MRCIS (blue) computations to visualize similarities and differences of the respective minima and conical intersections.

Table 3: Cremer-Pople parameters Q (dimensionless), θ and ϕ (degree) for the distortions of the six-membered ring, and the respective conformer classification according to Boeyens, of the optimized gas phase structures of the following 9*H*-guanine species: $(S_0)_{min}$, $(S_1)_{min}$, $CI_{01,\alpha}$, $CI_{01,\beta}$, and $CI_{01,\gamma}$. OM2/MRCI and MRCIS results from References 31 and 32, respectively.

	Q / Å	θ / °	ϕ / °	Conf.	Method
$CI_{01,\alpha}$	0.33	77	36	$^1S_2$	OM2/MRCI
	0.65	73	61	$B_{2,5}$	MRCIS
$CI_{01,\beta}$	0.51	61	64	E_2	OM2/MRCI
	0.51	58	58	E_2	MRCIS
$CI_{01,\gamma}$	0.42	44	310	E_6	OM2/MRCI
	0.61	58	332	$^1S_6$	MRCIS

Turning to the conical intersections, OM2/MRCI and MRCIS yield similar structures for $\mathbf{CI}_{01\beta}$ as can be seen by visual inspection (Figure 2e) and from the values of the optimized geometrical parameters (Table 2) and Cremer-Pople parameters (Table 3). The deviations are larger for the other two CI_{01} structures, which show stronger distortions at the MRCIS level (see Cremer-Pople parameter Q in Table 3). In the case of $\mathbf{CI}_{01\alpha}$, major deviations are found for the C4-C5 bond length (0.13 Å), the C2-N3-C4 bond angle (13°), and the N2-C2-N1-C6 dihedral angle (32°), with a much more pronounced boat-like distortion in MRCIS (Figure 2d). In the case of $\mathbf{CI}_{01\gamma}$, the N1-C6 bond is lengthened by more than 0.4 Å at the MRCIS level compared with OM2/MRCI (2.07 vs. 1.64 Å) and appears to be almost dissociated, with some concomitant changes in the bond angles around the C6=O6 carbonyl group, but otherwise the OM2/MRCI and MRCIS geometries are reasonably close to each other (Figure 2f).

4 Survey of literature data

Table 4: Excited-state lifetimes for 9*H*-guanine and its derivatives

Aqueous Solution	(pH=7)	
compound	life time	ref.
Gua	5 ps, 81 ps	Exp. by Fujiwara *et. al.*[15]
Guo	4 ps	Exp. by Fujiwara *et. al.*[15]
GMP	4 ps	Exp. by Fujiwara *et. al.*[15]
Guo	0.46 ps	Exp. by Pecourt *et. al.*[16,17]
Guo	0.69 ps	Exp. by Peon *et. al.*[18]
GMP	0.86 ps	Exp. by Peon *et. al.*[18]
dGuo	0.16 ps, 0.78 ps	Exp. by Onidas *et. al.*[19]
dGMP	0.20 ps, 0.89 ps	Exp. by Onidas *et. al.*[19]
dGMP	0.16-0.29 ps, 0.94-4.0 ps	Exp. by Miannay *et. al.*[20]
GMP	0.2 ps, 0.9 ps	Exp. by Karunakaran *et. al.*[21]
Gua	1.1-12.1 ps	Cal. by Doltsinis *et. al.*[13]
Gua	0.31 ps	Current calculations
Gas Phase		
compound	life time	ref.
Gua	0.8 ps	Exp. by Kang *et. al.*[14]
Gua	0.15 ps, 0.36 ps	Exp. by Canuel *et. al.*[11]
Gua	0.22 ps	Cal. by Barbatti *et. al.* at MRCIs level[32]
Gua	0.19 ps, 0.4 ps	Cal. by Lan *et. al.* at OM2/MRCI level[31]
Gua	0.8 ps	Cal. by Doltsinis *et. al.* at AIMD level[13]
9-Me-Gua	0.7-8.1 ps	Cal. by Langer *et. al.* at ROKS level[50,51]

5 Hydrogen bonding

5.1 Hydrogen bonding in the ground state

We determined the number of hydrogen bonds in the ground state of solvated 9*H*-guanine in two ways to validate our simulation setup. First we measured the radial distribution functions (RDFs) around the proton acceptor sites O6, N3 and N7 and around the proton donor sites N1-H, N2-H1, N2-H2 and N9-H from a ground-state QM/MM MD run (200 frames). RDFs were computed for bins of width 0.05 Å. Integration of the first peak of each RDF and summation over all hydrogen bonding sites resulted in an average coordination of 5.5 water molecules. This is smaller than the value of 8.5 observed in ground-state Car-Parrinello MD (CPMD) simulations with the BLYP functional.[64] The RDF plots are shown in Figure 3 separately for the proton donor and acceptor sites. The position (r) and height (g) of the first peak of each RDF are given in Table 5 both for the QM/MM MD and CPMD simulations. The first RDF

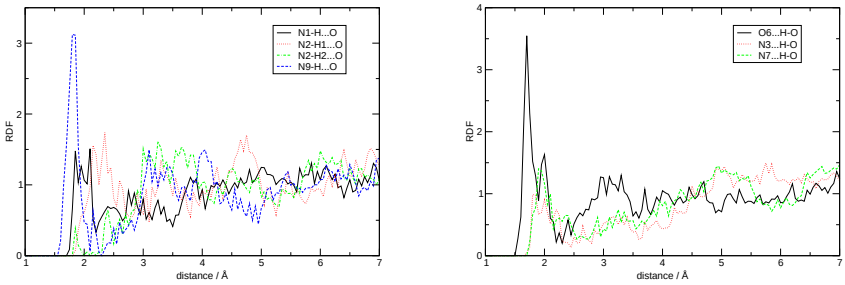

(a) proton donor sites (b) proton acceptor sites

Figure 3: RDF plots from ground-state QM/MM MD simulations of 9*H*-guanine in aqueous solution.

Table 5: Position (r in Å) and height (g) of the first maximum of each RDF for all donor and acceptor sites as obtained from QM/MM MD (this work) and CPMD simulations.[64]

site	QM/MM		CPMD	
	r_{max}	g_{max}	r_{max}	g_{max}
O6	1.7	3.55	1.9	2.09
N3	1.85	0.97	1.9	1.27
N7	1.9	1.4	1.8	1.3
N1-H	1.85	1.48	1.85	1.45
N2-H1	2.15	1.56	1.95	1.02
N2-H2	1.85	0.39	1.9	1.11
N9-H	1.8	3.12	1.85	1.43

peak occurs in most cases at similar hydrogen-bonding distances (typically around 1.9 Å), except for the QM/MM results at sites O6 and N2H1 (shorter and longer by about 0.2 Å, respectively). The peak heights are also often comparable (e.g., at sites N3, N7, and N1-H); they are more (less) pronounced in the QM/MM plots for sites O6 and N9-H (N2-H2). Visual inspection shows that the overall RDF plots from both sets of simulations are reasonably similar.

In addition, we studied the number of water molecules bound via hydrogen bonds in the QM/MM optimized geometries of ground-state 9*H*-guanine in water, for the five selected snapshots (see main text). This was done for the same hydrogen bonding sites as above (see Table 5). A hydrogen bond was assumed to exist if the relevant H...O or H...N distance was less than 2.5 Å and the associated O-H...O/N or N-H...O angle was larger than 150°. Water molecules bound to 9*H*-guanine via two hydrogen bonds were only counted once. Applying these criteria we identified seven (six) hydrogen-bonded water molecules in three (two) of the QM/MM optimized ground-state minima, which corresponds to an average of 6.7 hydrogen bonds.

5.2 Hydrogen bonding at the hopping points

Table 6: Average minimum distances from O6 to the closest lying hydrogen atom of the surrounding water molecules at the optimized minima and at the hopping points of set B (see text).

state	minimum O6-H distance / Å
$(S_0)_{min}$	1.67
$(S_{1\alpha})_{min}$	1.67
$(S_{1\beta})_{min}$	1.70
at hopping (a), boat like distortions	1.69
at hopping (b), NH_2 oop	1.87
at hopping (c), O6 oop	1.76
at hopping (d), distorted planes	1.75
at hopping, average	1.76

It should be noted that the minimum distance between the O6 atom and the closest hydrogen atom of the surrounding water molecules strongly fluctuates during the trajectory calculations. This is illustrated in Figure 4.

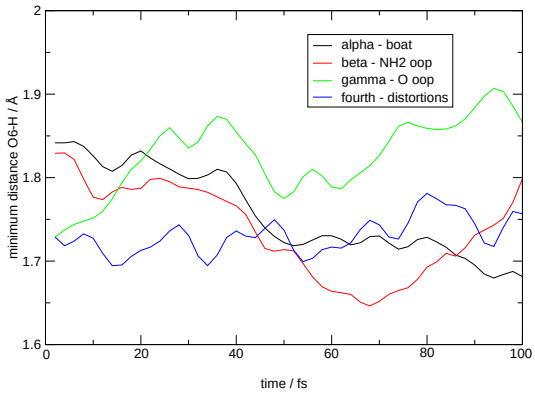

Figure 4: Time evolution of the minimum O6-hydrogen distance at the last 100 fs before hopping, averaged over five trajectories with the same hopping structure.

6 Geometrical Data

In this section, optimized Cartesian coordinates are given for all types of minima and conical intersections of 9*H*-guanine in aqueous solution (in Å). For each minimum or conical intersection, the structure of one typical representative snapshot is presented, as all structures of a given type are very close to each other.

- Ground-state minimum: $(S_0)_{min}$
- Excited-state minima: $(S_1)_{min,\alpha}$ and $(S_1)_{min,\beta}$
- Conical intersections: $CI_{01,\alpha}$, $CI_{01,\beta}$, $CI_{01,\gamma}$, and CI_{12}

$(S_0)_{min}$,	Figure 1 of the main paper		
N	-0.1144650200	-3.2589599300	-1.6151250100
C	0.2420168700	-1.9728369000	-1.3338678100
N	-0.6036851400	1.2699820100	-0.2450995000
H	-0.1838958500	2.1648091100	-0.0463262700
H	-1.5660436200	1.1646369900	0.0072454600
N	-0.5508577700	-0.9717393900	-0.8715152000
C	0.0998578600	0.2031031000	-0.6913740000
N	1.4455987200	0.3857294100	-0.9634313600
H	1.8693921600	1.3108224200	-0.8075985000
C	2.3047529300	-0.6301411600	-1.3978937500
O	3.5244230600	-0.3828570300	-1.5624941800
C	1.6528082800	-1.8893129400	-1.6236447100
N	2.0950024000	-3.1134358300	-2.0626089400
C	1.0266780100	-3.9173614400	-2.0507375200
H	1.0105444700	-4.9608917300	-2.3277186900
H	-1.0345320400	-3.7078838800	-1.4773532600

$(S_1)_{min,\alpha}$,	Figure 2a of the main paper		
N	0.0200354800	-3.2479173600	-2.0756461200
C	0.3681553000	-1.9336853400	-1.8183599900
N	-0.3046479200	1.0815612100	-0.2227668200
H	-0.0148178600	2.0515973200	-0.1876497700
H	-1.0839850900	0.8087132900	0.3425910000
N	-0.3911348000	-1.0068583800	-1.2328036500
C	0.2627108700	0.2056455800	-1.0722961100
N	1.4041062800	0.5814532700	-1.7322870000
H	1.8458492600	1.4489184100	-1.4238196600
C	2.2881065100	-0.3516516900	-2.4490746200
O	3.4395763500	-0.5000118200	-1.9652808600
C	1.4940488600	-1.6629237300	-2.7521923400
N	1.8532827600	-2.8105364100	-3.3126242800
C	0.9777867600	-3.7658640000	-2.9054954600
H	0.9494124200	-4.7646124100	-3.2942345500
H	-0.7285666300	-3.7909518400	-1.6328836200

$(S_1)_{min,\beta}$,	Figure 2b of the main paper		
N	0.1993825400	-3.0560382100	-1.9397799700
C	0.4381702800	-1.8377169400	-1.3151832300
N	-0.3127211800	1.3627405400	-0.1373820400
H	0.0252480700	2.3126159300	-0.0851260800
H	-1.2062883200	1.1992014400	0.2829624300
N	-0.3749310300	-0.8814030800	-1.0228323000
C	0.4342123000	0.3243079400	-0.5291535400
N	1.6267321100	0.6318589000	-1.2385851800
H	1.9246631500	1.5842869700	-1.4487574800
C	2.5005278000	-0.4019769300	-1.4538791600
O	3.6676403900	-0.2157754300	-1.8788281300
C	1.9496332700	-1.7610235300	-1.2512151600
N	2.4402186200	-2.8750843700	-1.8454500400
C	1.4100760000	-3.6865582000	-2.1226880200
H	1.4932377600	-4.7172838200	-2.4662023900
H	-0.7202765200	-3.5255322700	-1.9815731800

$CI_{01,\alpha}$,	Figure 3a of the main paper		
N	-0.1274377	-3.1754855	-2.4453567
C	-0.0427515	-2.0131867	-1.6248297
N	-0.8031812	1.0709141	-0.0890641
H	-0.5536385	2.0473114	-0.0329880
H	-1.6882751	0.8138663	0.3218832
N	-0.8864554	-1.1110492	-1.4098692
C	-0.0216660	0.1099868	-0.5498985
N	1.2036383	0.4680395	-1.1247941
H	1.5398083	1.4150237	-1.2843137
C	2.0519693	-0.5818408	-1.3922790
O	3.2406162	-0.3967134	-1.7189635
C	1.4732137	-1.9624453	-1.3009431
N	2.0583053	-2.9902054	-1.9533351
C	1.0925384	-3.7957449	-2.4254536
H	1.2462041	-4.8209109	-2.7795654
H	-1.0069117	-3.7000942	-2.5049857

$CI_{01,\beta}$,	Figure 3b of the main paper		
N	0.2013367	-3.5896853	-1.4947628
C	0.0731136	-2.2314323	-1.2976006
N	0.1117894	-0.3321526	0.7101136
H	0.8248420	0.2990149	1.0453884
H	-0.2259926	-1.0173176	1.3613462
N	-0.9890799	-1.4639477	-1.0472516
C	-0.4198263	-0.2528068	-0.5455265
N	0.3589274	0.4828939	-1.4860964
H	0.3378592	1.5141398	-1.4990036
C	1.4411401	-0.2038108	-1.9762874
O	2.3664765	0.3288124	-2.6420660
C	1.3667088	-1.6590117	-1.7329144
N	2.1386046	-2.6643549	-2.1980499
C	1.4564395	-3.8111619	-2.0244642
H	1.8380017	-4.7941307	-2.2621094
H	-0.4838777	-4.2947042	-1.2098314

$CI_{01,\gamma}$,	Figure 3c of the main paper		
N	0.1413053	-4.2958087	-1.1415238
C	0.5145724	-2.9707623	-1.2781192
N	-0.3475526	0.4051143	-1.0944890
H	-0.0580912	1.3412088	-1.3468788
H	-1.2240711	0.3282307	-0.6150457
N	-0.2969247	-1.9152186	-1.2348219
C	0.3315682	-0.6995299	-1.4498274
N	1.5413758	-0.5878975	-2.0871962
H	1.9400696	0.3555970	-2.1407156
C	2.5402336	-1.6593842	-1.8803881
O	3.2251093	-1.5278629	-0.8320011
C	1.8295938	-3.0310094	-1.9877061
N	2.2271193	-4.2957069	-2.0155236
C	1.2300529	-5.0554315	-1.4874983
H	1.2751511	-6.1244426	-1.3767666
H	-0.6952950	-4.6323605	-0.6483259

CI_{12},	Figure 4 of the main paper		
N	-0.1010613	-3.3888893	-1.5498091
C	-0.1896241	-2.0285463	-1.3235422
N	-1.8035112	0.8096283	-0.1557756
H	-1.7394570	1.8096891	-0.0970849
H	-2.5769638	0.3751669	0.3120401
N	-1.2633530	-1.2637184	-1.1681708
C	-0.8707441	0.0552308	-0.7558956
N	0.1946983	0.7049205	-1.4063670
H	0.3442341	1.7030350	-1.2079468
C	1.3387557	-0.0276196	-1.7564875
O	2.4846693	0.4570414	-1.6088778
C	1.1242049	-1.4993131	-1.7601755
N	1.8932510	-2.5170714	-2.1506933
C	1.1879224	-3.6603761	-1.9674384
H	1.5597635	-4.6452506	-2.2053182
H	-0.7770096	-4.0882618	-1.2278522